Myocardial Acceleration Calculation from Highly Time Resolved Tissue Phase Mapping

F. Staehle[1], B. A. Jung[1], D. Föll[1], E. Schilli[1], J. Hennig[1], and M. Markl[1]
[1]Department of Diagnostic Radiology, University Hospital Freiburg, Freiburg, Germany

Introduction: Tissue Phase Mapping (TPM) has proven to be a robust tool for the assessment of myocardial motion [1], [2]. However, little has been reported about the calculation of acceleration data from velocity TPM data derivatives [3]. The acceleration vector field might yield information about the structure of heart muscle fibers and may provide new insights into the nature and extent of various cardiac diseases. Recently reported advances in TPM providing high temporal resolution data (13.8 ms) offer the opportunity to derive myocardial acceleration for the velocity data. In this study, a strategy for the calculation of local and global myocardial acceleration from highly time resolved TPM velocity data is presented.

Methods: Measurements: All measurements were performed on a 1.5T MR-system (Sonata, Siemens, Germany). Data were acquired using a 2D phase contrast sequence with three-directional velocity encoding and black blood saturation [4]. The temporal resolution was 13.8 ms, other imaging parameters as in [4].
Volunteers and Patients: 10 Volunteer were included: 8 volunteers in the age group between 20 and 40 years, one 50-year-old volunteer, and one 62 year-old-volunteer. Two patients were included in the analysis. One 59-year-old male patient suffered from aortic insufficiency (ejection fraction = 50%). The other 64-year-old male patient suffered from a cardiomyopathy (ejection fraction = 40%).
Acceleration Calculation: For the calculation of myocardial acceleration acc(t) of a specific cardiac phase t the previous cardiac time farme t-Δt and the successive time frame t+Δt were used (Δt = temporal resolution). First, inner and outer myocardial contours of all time-frames were manually segmented and corrected for the global heart motion as described previously [4]. Next, each voxel with the segmentation contours at time frame t was tracked to its position at t-Δt and t+Δt (Figure 1). The average contribution to the voxel was taken as the corresponding velocity value at t-Δt and t+Δt, respectively [5], [6]. Based on a coordinate transformation to a heart-intrinsic coordinate system, the acceleration at time t was calculated from the three cardiac time frames by a non-linear curve fit to the three points and evaluating the derivative at t to calculate the accelerations in the radial direction (a_r), in the tangential direction (a_{phi}) and in the long-axis-direction (a_z).
Data analysis: The duration of systole was defined as the initial time period with positive radial velocities v_r. To analyze differences in myocardial acceleration peak systolic and diastolic acceleration and deceleration as well as time to peak (TTP) to the corresponding peaks were determined (see also Fig. 2).

Results: Time-resolved average myocardial acceleration components a_r, a_{phi} and a_z of the heart funcion for the eight young volunteers are shown in figure 2. The top row shows the directly measured velocities, the bottom row the derived accelerations in the heart-intrinsic coordinate system (Fig. 1). For each axis location, data were averaged over the segmented left ventricle and all volunteers. Figure 3 shows the results of two patient measurements, compared with the average time course of the 8 healthy volunteers for the average radial and long-axis velocity and acceleration for a midventricular slice. The difference between the pathological and helthy heart motion is evident from both the velocity and acceleration plots.
Figure 4 shows the color-coded acceleration maps of the healthy 62-year-old volunteer (a) and (b), the patient suffering from an aortic insufficiency (c), and the patient suffering from a cardiomyopathy (d). The images depict normal maximum systolic acceleration and maximum diastolic acceleration (a and b) for the volunteer and maximum diastolic acceleration for the patients (c and d). The patients' acceleration maps show abnormalities in the lateral region.
Results of peak and TTP acceleration analysis are summarized in table 1. From table 1 can be inferred that the radial diastolic acceleration and both the radial and the longitudinal deceleration were lower in the patients than in the volunteers:

Volunteers	Peak radial acc - systole [cm/s²]	Peak radial dec - systole [cm/s²]	Peak radial acc - diastole [cm/s²]	Peak radial dec - diastole [cm/s²]	Peak long-axis acc - systole [cm/s²]	Peak long-axis dec - systole [cm/s²]	Peak long-axis acc - diastole [cm/s²]	Peak long-axis dec - diastole [cm/s²]
20 – 40 years	62.9 ± 11.0	-76.1 ± 19.7	-100.0 ± 32.8	138.4 ± 45.8	129.2 ± 42.6	-111.3 ± 17.2	-156.1 ± 50.4	285.3 ± 88.5
52 years	56.8	-67.5	-116.2	98.2	55.0	-84.5	-101.7	139.8
60 years	49.8	-72.2	-76.3	75.0	105.8	-74.4	-86.3	116.5
Patients								
Aortic insuff.	68.0	-66.4	-28.1	18.9	140.9	-49.8	-135.7	95.8
Cardiomyopathy	45.0	-58.0	-52.2	39.6	123.6	-82.9	-95.2	55.0

Volunteers	Radial TTP acc - systole [ms]	Radial TTP dec - systole [ms]	Radial TTP acc - diastole [ms]	Radial TTP dec - diastole [ms]	Long-axis TTP acc - systole [ms]	Long-axis TTP dec - systole [ms]	Long-axis TTP acc - diastole [ms]	Long-axis TTP dec - diastole [ms]
20 – 40 years	39.7 ± 20.8	289.8± 25.6	376.1 ± 57.0	464.0 ± 23.8	34.5 ± 22.1	69.0 ± 25.6	350.2 ± 38.6	462.3 ±2 0.9
52 years	20.7	269.1	379.5	434.7	20.7	89.7	338.1	448.5
60 years	35.5	269.1	393.3	476.1	20.7	62.1	324.3	462.3
Patients								
Aortic insuff.	20.7	269.1	420.9	310.5	20.7	75.9	296.7	572.7
Cardiomyopathy	35.5	282.9	434.7	476.1	20.7	62.1	345	483

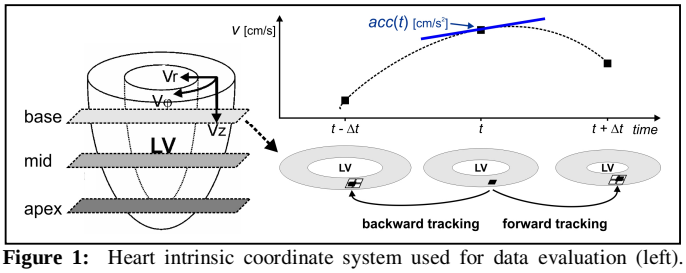

Figure 1: Heart intrinsic coordinate system used for data evaluation (left). Bottom right: Voxel motion was tracked within the segmented LV in a specific plain by determining the voxel's position at times t±Δt. Top right: The tangent to the fitted curve at time t was taken as the acceleration acc(t) at time t.

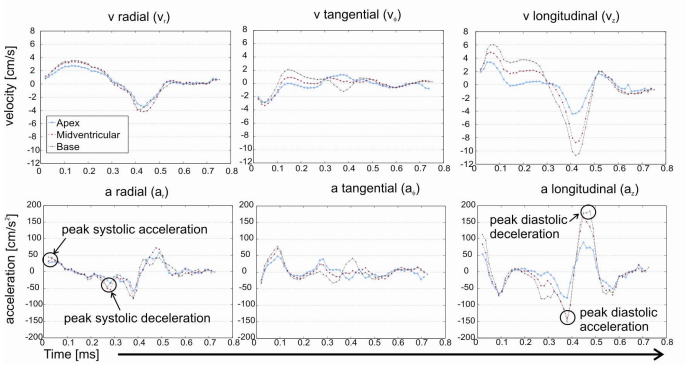

Figure 2: Average velocity (top row) and acceleration (bottom row) graphs of the basal (black lines), midventricular (red lines) and apical (blue lines) slices for eight volunteers (age = 20 - 40 years).

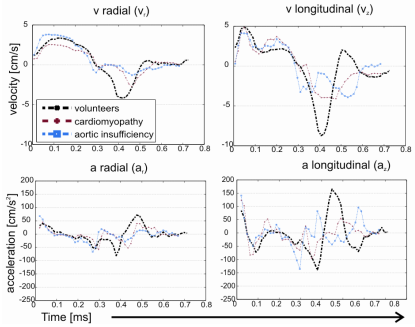

Figure 3: Velocity and acceleration graphs for a patient with aortic insufficiency (blue line) and a patient with a cardiomyopathy (red line) of a midventricular slice. The black line represents the group of eight volunteers of age 20 – 40.

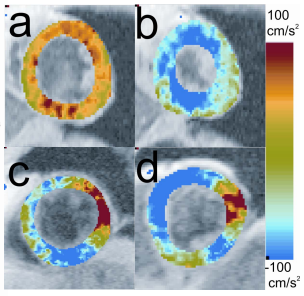

Figure 4: Color-coded acceleration maps of a midventricular slice of the left ventricular myocardium. (a) cardiac phase with maximum systolic acceleration for a 62 year-old healthy volunteer. (b) maximum diastolic acceleration for the same volunteer, (c) for the patient with aortic insufficiency, (d) for the patient with cardiomyopathy.

Discussion: The results of this study demonstrate the feasibility of the evaluation of myocardial acceleration data from high temporal-resolution TPM-velocity data. Since acceleration is related to the force, acceleration might yield valuable information about the performance of the left ventricular myocardium. From table 1 it can be inferred that the peak diastolic acceleration in the radial direction and peak diastolic deceleration in the longitudinal direction is lower for both patients than for the volunteers. Interestingly, both patients demonstrated increased systolic peak longitudinal accelerations compared to the healthy volunteers, despite suffering from a depressed global left ventricle, whereas diastolic peak acceleration was reduced in the patient with dilative cardiomyopathy and rather enhanced in the patient with aortic insufficiency. This stresses the fact, that global ejection fraction does not adequately reflect the contractile forces inherent in the heart muscle. In future studies, a larger number of volunteers and patients have to be included and a comparison with TPM data acquired with acceleration encoding may provide additional valuable information.

References: [1] Markl et al., JMRI 2002; 15(6):642-53 [2] Kvitting et al., J Cardiovasc Magn Reson 2004;6(3):627-636 [3] Jung et al., Eur J Cardiothorac Surg 2006; 29:158-164 [4] Jung et al., JMRI 2006;24(5):1033-1039 [5] Pelc et al., Invest Radiol 1994;29:1038-1042 [6] Drangova et al., MRI 1998;16(8):863-870

Acknowledgements: Grant support by the Deutsche Forschungsgemeinschaft (DFG), Grant # HE 1875/18-1, and the Bundesministerium für Bildung und Forschung (BMBF), Grant # 01EV0706.